

## Communication

# A straightforward method for stereospecific assignment of val and leu prochiral methyl groups by solid-state NMR: Scrambling in the [2-<sup>13</sup>C]Glucose labeling scheme

Guohua Lv, Hannes Klaus Faßhuber, Antoine Loquet, Jean-Philippe Demers, Vinesh Vijayan, Karin Giller, Stefan Becker, Adam Lange\*

Max Planck Institute for Biophysical Chemistry, Department of NMR-based Structural Biology, Am Fassberg 11, 37077 Göttingen, Germany

## ARTICLE INFO

## Article history:

Received 5 November 2012

Revised 19 December 2012

Available online 4 January 2013

## Keywords:

Solid-state NMR

Stereospecific assignment

Sparse labeling

## ABSTRACT

The unambiguous stereospecific assignment of the prochiral methyl groups in Val and Leu plays an important role in the structural investigation of proteins by NMR. Here, we present a straightforward method for their stereospecific solid-state NMR assignment based on [2-<sup>13</sup>C]Glucose ([2-<sup>13</sup>C]Glc) as the sole carbon source during protein expression. The approach is fundamentally based on the stereoselective biosynthetic pathway of Val and Leu, and the co-presence of [2-<sup>13</sup>C]pyruvate produced mainly by glycolysis and [3-<sup>13</sup>C]/[1,3-<sup>13</sup>C]pyruvate most probably formed through scrambling in the pentose phosphate pathway. As a consequence, the isotope spin pairs <sup>13</sup>Cβ-<sup>13</sup>Cγ2 and <sup>13</sup>Cα-<sup>13</sup>Cγ1 in Val, and <sup>13</sup>Cγ-<sup>13</sup>Cδ2 and <sup>13</sup>Cβ-<sup>13</sup>Cδ1 in Leu are obtained. The approach is successfully demonstrated with the stereospecific assignment of the methyl groups of Val and Leu of type 3 secretion system PrgI needles and microcrystalline ubiquitin.

© 2012 Elsevier Inc. All rights reserved.

## 1. Introduction

The stereospecific assignment of prochiral methyl groups of Val and Leu can greatly improve the precision and accuracy in protein structure determination by liquid-state NMR [1–4]. The methyl groups of Leu and Val are useful sources of structural information, as they are often found abundantly in the structurally important hydrophobic protein core and involved in numerous inter-residue and long-range contacts [5]. Additionally, it was recently shown that the methyl carbon chemical shifts can be used for obtaining  $\chi_1$  rotamer distributions in Val and Leu residues, and that the methyl groups are a rich source of information about side-chain conformation and dynamics [6,7]. ssNMR spectroscopy is an emerging powerful tool for the structure determination of non-crystalline and insoluble proteins [8–12], which are not amenable to X-ray crystallography or solution NMR spectroscopy. The stereospecific assignment of the prochiral methyl groups of Val and Leu by ssNMR, should play an equally important role for structural and dynamical studies as in liquid-state NMR.

In order to address the stereospecific assignment of the prochiral methyl groups of Val and Leu, several isotope-labeling approaches have been developed [2,3,13–17]. The most widely used method to date relies on the use of a minimal culture

medium containing 10% [<sup>13</sup>C]Glucose and 90% [<sup>12</sup>C]Glucose as the carbon source during biosynthetic protein production [2,18,19]. This elegant method has been successfully applied for obtaining the stereospecific assignment of the isopropyl groups of Val and Leu by liquid-state NMR and has also been extended to ssNMR [20]. However, a major practical drawback of this method is that the fractional labeling requires an additional sample to be prepared only for the purpose of stereospecific assignments.

Here, we propose an alternative approach for the stereospecific assignment of the methyl groups of Val and Leu based on the [2-<sup>13</sup>C]Glucose ([2-<sup>13</sup>C]Glc) labeling scheme. Bacterial growth in media containing [2-<sup>13</sup>C]Glc results in high <sup>13</sup>C spin dilution in the protein produced with only one out of six carbons labeled [21,22]. We have reported earlier that the [2-<sup>13</sup>C]Glc labeling scheme leads to a significant resolution enhancement in ssNMR spectra and also to improvements in polarization transfer efficiencies due to the reduction of dipolar truncation effects [21,23]. In combination with uniformly [<sup>13</sup>C]Glc labeled ([U-<sup>13</sup>C]Glc-labeled) and [1-<sup>13</sup>C]Glc-labeled samples, sequential resonance assignments can be readily obtained [23]. Herein, we present that the [2-<sup>13</sup>C]Glc labeling scheme additionally allows for obtaining stereospecific assignments of the isopropyl groups of Val and Leu in a straightforward manner using ssNMR spectroscopy. As an illustration, we present stereospecific assignments of Val and Leu in type 3 secretion system (T3SS) PrgI needles and microcrystalline ubiquitin.

\* Corresponding author.

E-mail address: [adla@nmr.mpibpc.mpg.de](mailto:adla@nmr.mpibpc.mpg.de) (A. Lange).

## 2. Results and discussion

The  $^{13}\text{C}$  enrichment pattern of  $[2-^{13}\text{C}]\text{Glc}$  has been well established by Lundström et al. [22]. To further investigate the labeling pattern and possible scrambling, we recorded a  $^1\text{H}-^{13}\text{C}$  HSQC spectrum of T3SS PrgI protomers that were produced with  $[2-^{13}\text{C}]\text{Glc}$  as the sole carbon source. As shown in Fig. S1, the observation of  $^{13}\text{C}\gamma_1/2$  of Val,  $^{13}\text{C}\delta_1/2$  of Leu, and  $^{13}\text{C}\beta$  of Ala with strong intensity indicates that metabolic scrambling indeed occurred. Starting from glucose, glycolysis leads to pyruvate as its final product (Fig. S2a) [24]. As a consequence, about 50%  $[2-^{13}\text{C}]\text{pyruvate}$  is expected when starting from  $[2-^{13}\text{C}]\text{Glc}$ . As an alternative pathway to glycolysis, the pentose phosphate pathway (PPP) [24] yields  $[1-^{13}\text{C}]/[1,3-^{13}\text{C}]\text{Fructose-6-phosphate}$  (F6P) and  $\text{Glyceraldehyde-3-phosphate}$  (GAP) starting from  $[2-^{13}\text{C}]\text{Glucose-6-phosphate}$  (G6P; Fig. S2b). The resulting F6P and GAP may reenter glycolysis and also yield pyruvate [24,25], with  $[1-^{13}\text{C}]\text{F6P}$  and  $[1,3-^{13}\text{C}]\text{F6P}$  leading to the formation of  $[3-^{13}\text{C}]\text{pyruvate}$  and  $[1,3-^{13}\text{C}]\text{pyruvate}$ , respectively. It is believed that the PPP constitutes the most important alternative pathway that can ultimately yield pyruvate in addition to glycolysis [26,27]. Additionally, the  $[2-^{13}\text{C}]\text{F6P}$  obtained during glycolysis may also be converted to  $[2-^{13}\text{C}]\text{Ribose-5-phosphate}$  (R5P) and  $[2-^{13}\text{C}]\text{Xylulose-5-phosphate}$  (Xu5P) (see reactions 1–5 in Fig. S2), which can then be converted to  $[2-^{13}\text{C}]\text{F6P}$  and  $[2,3-^{13}\text{C}]\text{F6P}$  (via reactions 3–4 or 5; see Fig. S2). Subsequently,  $[2-^{13}\text{C}]\text{pyruvate}$  and  $[1,2-^{13}\text{C}]\text{pyruvate}$  can be formed.

Moreover, the biosynthesis of Val and Leu from pyruvate is stereoselective [2,18–20], i.e., the Pro-R methyl carbon ( $\text{C}\gamma_1$  in Val and  $\text{C}\delta_1$  in Leu) derives from the same pyruvate as the adjacent branching methine carbon, while the Pro-S methyl carbon ( $\text{C}\gamma_2$  in Val and  $\text{C}\delta_2$  in Leu) derives from a separate pyruvate. As a consequence, with the presence of the above mentioned isotopomers of pyruvate, e.g.,  $[2-^{13}\text{C}]\text{pyruvate}$  and  $[3-^{13}\text{C}]\text{pyruvate}$ , only the Pro-S methyl carbon is  $^{13}\text{C}$  enriched simultaneously with the directly bonded carbon, while the Pro-R carbon is  $^{13}\text{C}$  enriched simultaneously with the carbon two bonds apart ( $\text{C}\alpha$  in Val and  $\text{C}\beta$  in

Leu). As shown in Fig. 1, the labeled spin pairs  $^{13}\text{C}\beta-^{13}\text{C}\gamma_2$  and  $^{13}\text{C}\alpha-^{13}\text{C}\gamma_1$  in Val (Fig. 1a), and  $^{13}\text{C}\gamma-^{13}\text{C}\delta_2$  and  $^{13}\text{C}\beta-^{13}\text{C}\delta_1$  in Leu (Fig. 1b) are obtained. Thus, by means of  $^{13}\text{C}-^{13}\text{C}$  correlation ssNMR spectroscopy, the two prochiral methyl groups of Val and Leu can be readily distinguished and the stereospecific assignment obtained. The resulting  $^{13}\text{C}-^{13}\text{C}$  correlation spectrum will exhibit strong intensity correlations for  $^{13}\text{C}\beta-^{13}\text{C}\gamma_2$  and  $^{13}\text{C}\alpha-^{13}\text{C}\gamma_1$  of Val, and  $^{13}\text{C}\gamma-^{13}\text{C}\delta_2$  and  $^{13}\text{C}\beta-^{13}\text{C}\delta_1$  of Leu, respectively. In contrast, the correlations  $^{13}\text{C}\alpha-^{13}\text{C}\gamma_2$  and  $^{13}\text{C}\beta-^{13}\text{C}\gamma_1$  of Val, and  $^{13}\text{C}\beta-^{13}\text{C}\delta_2$  and  $^{13}\text{C}\gamma-^{13}\text{C}\delta_1$  of Leu are not expected. In case of a crowded methyl region in  $^{13}\text{C}-^{13}\text{C}$  correlation ssNMR spectra, this method thus bears another advantage, i.e., the simplification by the decreased number of detected correlations, in addition to the spectroscopic differentiation of the prochiral methyl groups.

The stereospecific  $^{13}\text{C}$  labeling pattern of Val and Leu resulting from  $[2-^{13}\text{C}]\text{Glc}$  is successfully demonstrated with applications to T3SS PrgI needles (Fig. 2a) and ubiquitin (Fig. S4), where stereospecific assignments of Val and Leu are obtained unambiguously. As shown in Fig. 2a, generally only one methyl carbon ( $^{13}\text{C}\gamma_1$  or  $^{13}\text{C}\gamma_2$ ) correlates to  $^{13}\text{C}\alpha$  or  $^{13}\text{C}\beta$  of Val in the 2D  $^{13}\text{C}-^{13}\text{C}$  PDS spectrum of  $[2-^{13}\text{C}]\text{Glc}$ -labeled T3SS PrgI needles (in magenta), while four correlations ( $^{13}\text{C}\gamma_1/2-^{13}\text{C}\beta$  and  $^{13}\text{C}\gamma_1/2-^{13}\text{C}\alpha$ ) are present in the 2D PDS spectrum of  $[\text{U}-^{13}\text{C}]\text{Glc}$ -labeled T3SS PrgI needles (in black). For Val12, 27, and 65, as expected, the correlations of  $^{13}\text{C}\alpha-^{13}\text{C}\gamma_1$  and  $^{13}\text{C}\beta-^{13}\text{C}\gamma_2$  were observed for  $[2-^{13}\text{C}]\text{Glc}$ -labeled T3SS PrgI needles (magenta spectrum in Fig. 2a). For Val20, only the correlation of  $^{13}\text{C}\alpha-^{13}\text{C}\gamma_1$  was observed, but with weak intensity, while the correlation of  $^{13}\text{C}\beta-^{13}\text{C}\gamma_2$  was absent. This observation is consistent with the observation of weak-intensity correlations in the 2D PDS spectrum of  $[\text{U}-^{13}\text{C}]\text{Glc}$ -labeled T3SS PrgI needles (in black) and can be attributed to structural plasticity [10]. For Val67, in addition to the  $^{13}\text{C}\alpha-^{13}\text{C}\gamma_1$  and  $^{13}\text{C}\beta-^{13}\text{C}\gamma_2$  correlations, a  $^{13}\text{C}\alpha-^{13}\text{C}\gamma_2$  correlation was also observed, but with much weaker intensity compared to the expected correlations. Peaks that are observed in the  $[2-^{13}\text{C}]\text{Glc}$ -labeled spectrum in addition to the ones observed in the  $[\text{U}-^{13}\text{C}]\text{Glc}$ -labeled sample corre-

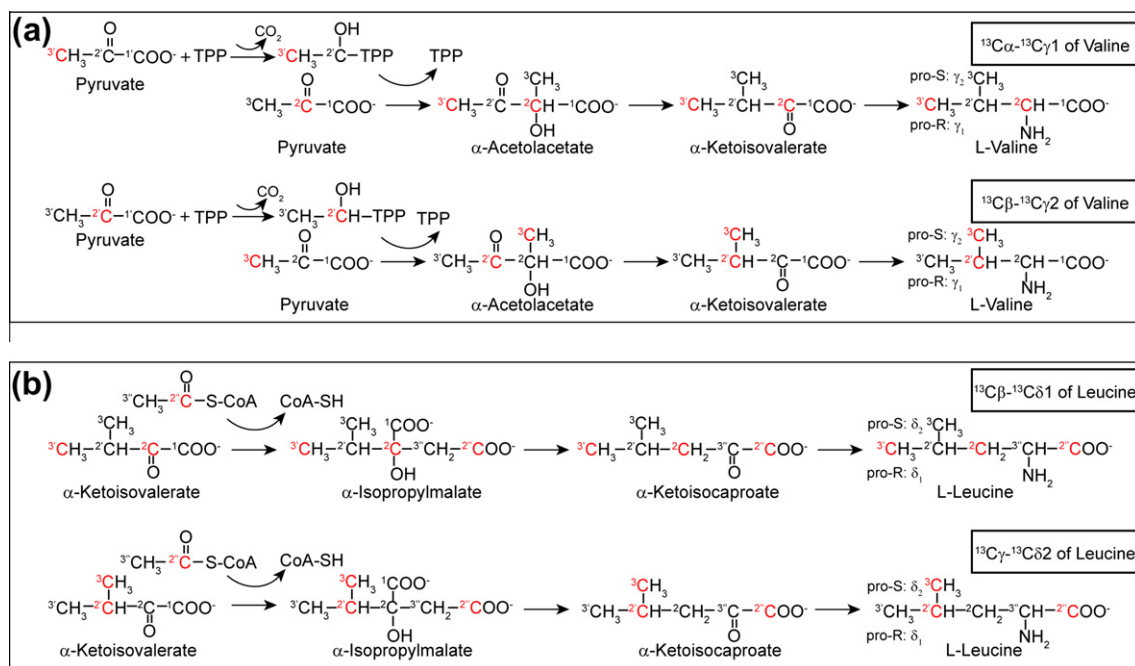


**Fig. 1.** The stereoselective biosynthesis of Val and Leu. As an example, the formation of the isotope pairs (a)  $^{13}\text{C}\alpha-^{13}\text{C}\gamma_1/^{13}\text{C}\beta-^{13}\text{C}\gamma_2$  of Val, and (b)  $^{13}\text{C}\beta-^{13}\text{C}\delta_1/^{13}\text{C}\gamma-^{13}\text{C}\delta_2$  of Leu originating from  $[2-^{13}\text{C}]\text{pyruvate}$  and  $[3-^{13}\text{C}]\text{pyruvate}$  is shown. The carbons that are  $^{13}\text{C}$  labeled are colored in red. Abbreviations: TPP, thiamine pyrophosphate; CoA: Coenzyme A.

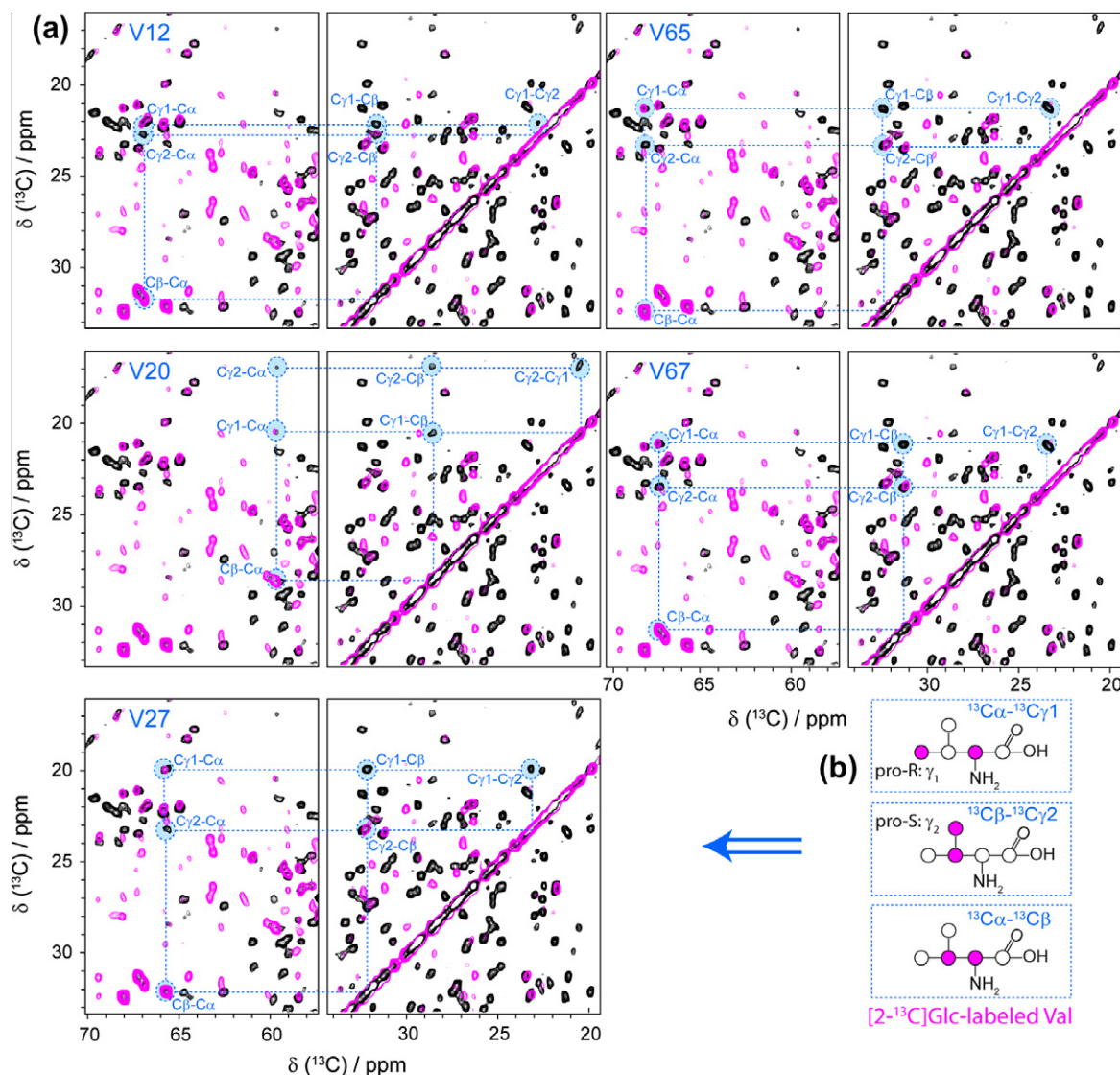


**Fig. 2.** (a) 2D PDSD spectra of [U- $^{13}\text{C}$ ]Glc- (in black) and [2- $^{13}\text{C}$ ]Glc-labeled (in magenta) T3SS PrgI needles. The spectrum of the [U- $^{13}\text{C}$ ]Glc-labeled sample was recorded with a mixing time of 50 ms, using maximum acquisition times of 20 ms (direct dimension) and 15 ms (indirect dimension). The total experimental time was 3 days. The spectrum of the [2- $^{13}\text{C}$ ]Glc-labeled sample was recorded with a mixing time of 400 ms, using maximum acquisition times of 15 ms (direct dimension) and 10 ms (indirect dimension). The total experimental time was 1.5 days. Spin systems for V12, V20, V27, V65, and V67 are highlighted in blue. The stereospecific assignment of  $^{13}\text{C}_{\gamma 1/2}$  in Val (a) was obtained based on the correlations  $^{13}\text{C}_{\alpha}-^{13}\text{C}_{\gamma 1}$  and  $^{13}\text{C}_{\beta}-^{13}\text{C}_{\gamma 2}$  as illustrated in (b). 1D slices for the residues Val65 and Val67 are shown in Fig. S3.

spond to sequential, medium- and long-range correlations, as the PDSD mixing time used was longer (400 ms).

Similarly for Leu, the stereoselective  $^{13}\text{C}$  enrichment pattern, i.e.,  $^{13}\text{C}_{\beta}-^{13}\text{C}_{\delta 1}$  and  $^{13}\text{C}_{\gamma}-^{13}\text{C}_{\delta 2}$ , is illustrated using [2- $^{13}\text{C}$ ]Glc-labeled ubiquitin (magenta spectrum in Fig. S4b). Taking Leu56 as an example, the correlations  $^{13}\text{C}_{\beta}-^{13}\text{C}_{\delta 1}$  and  $^{13}\text{C}_{\gamma}-^{13}\text{C}_{\delta 2}$  were observed without the presence of the correlations  $^{13}\text{C}_{\beta}-^{13}\text{C}_{\delta 2}$  and  $^{13}\text{C}_{\gamma}-^{13}\text{C}_{\delta 1}$ . However, for Leu50, only the correlation of  $^{13}\text{C}_{\gamma}-^{13}\text{C}_{\delta 2}$  was clearly present, while the correlation of  $^{13}\text{C}_{\beta}-^{13}\text{C}_{\delta 1}$  was very weak and only observable on one side of the diagonal. This might be due to the longer distance involved in this correlation (two bonds) compared to the  $^{13}\text{C}_{\gamma}-^{13}\text{C}_{\delta 2}$  (one bond) correlation. Additionally, strong  $^{13}\text{C}_{\beta}-^{13}\text{C}_{\gamma}$  cross-peaks are observed for Leu. These peaks are expected from the labeling pattern and are very intense compared to the  $^{13}\text{C}_{\gamma}-^{13}\text{C}_{\delta 2}$  and  $^{13}\text{C}_{\beta}-^{13}\text{C}_{\delta 1}$  peaks that are only observed due to scrambling.

In principle, one can directly identify Val and Leu methyl groups by their expected correlations in PDSD spectra of [2- $^{13}\text{C}$ ]Glc-labeled samples, i.e.,  $^{13}\text{C}_{\alpha}-^{13}\text{C}_{\gamma 1}$  and  $^{13}\text{C}_{\beta}-^{13}\text{C}_{\gamma 2}$  for Val, and

$^{13}\text{C}_{\beta}-^{13}\text{C}_{\delta 1}$  and  $^{13}\text{C}_{\gamma}-^{13}\text{C}_{\delta 2}$  for Leu. However, in case of absence of expected peaks, e.g., as seen in this study for PrgI Val20  $^{13}\text{C}_{\beta}-^{13}\text{C}_{\gamma 2}$ , one also needs [U- $^{13}\text{C}$ ]Glc spectra to assist the assignment of  $^{13}\text{C}_{\gamma 1/2}$ .

In addition to the scrambling due to the PPP detailed above, it is noteworthy that (a) amino acid degradation together with the  $\text{C}_1$  metabolism [24], (b) the breakdown of oxaloacetate via gluconeogenesis [24] as well as (c) the conversion of malate [24] might contribute to scrambling resulting in (a) [3- $^{13}\text{C}$ ]pyruvate, [1- $^{13}\text{C}$ ]pyruvate, [1,3- $^{13}\text{C}$ ]pyruvate, and [2,3- $^{13}\text{C}$ ]pyruvate, (b) [1,3- $^{13}\text{C}$ ]pyruvate and [1- $^{13}\text{C}$ ]pyruvate, and (c) [1,3- $^{13}\text{C}$ ]pyruvate and [1- $^{13}\text{C}$ ]pyruvate ([2- $^{13}\text{C}$ ]pyruvate is not considered here, as it is always present in the [2- $^{13}\text{C}$ ]Glc-labeling scheme). As mentioned above, the spin pairs  $^{13}\text{C}_{\beta}-^{13}\text{C}_{\gamma 1}$  and  $^{13}\text{C}_{\alpha}-^{13}\text{C}_{\gamma 2}$  of Val originate from carbons 2 and 3 of a single pyruvate (Fig. 1). Therefore, the presence of [2,3- $^{13}\text{C}$ ]pyruvate could explain the presence of the  $^{13}\text{C}_{\alpha}-^{13}\text{C}_{\gamma 2}$  correlation of Val67 in T3SS PrgI needles (Fig. 2a). However, consistent with the observed weak intensity, it was reported that amino acid degradation and gluconeogenesis are quite

generally of minor importance when *Escherichia coli* cells have access to glucose [24,28]. This implies that the enrichment level of [2,3-<sup>13</sup>C]pyruvate is so low that it does not disturb the stereospecific assignment of Val and Leu. This is also corroborated by the fact, that no Ala C $\alpha$ –C $\beta$  peaks are observed in ssNMR spectra of [2-<sup>13</sup>C]Glc-labeled proteins [21,23,29], which would be the case if [2,3-<sup>13</sup>C]pyruvate was present.

### 3. Conclusion

In conclusion, we have presented an alternative stereospecific labeling pattern of Val and Leu formed by the co-presence of [2-<sup>13</sup>C]pyruvate and [3-<sup>13</sup>C]/[1,3-<sup>13</sup>C]pyruvate starting from [2-<sup>13</sup>C]Glc, enabling us to obtain stereospecific assignments of the isopropyl groups of Val and Leu in a simple way. For this purpose, only a unique [2-<sup>13</sup>C]Glc-labeled sample is required, the isotope expense is thus reduced compared to fractional labeling approaches [2,18–20]. Given the resolution enhancement and spectral simplification that we have recently exploited for the *de novo* sequential assignment of the T3SS PrgI needles [23] and of mouse  $\alpha$ -synuclein fibrils [29], the detection of long-range distance restraints [10], and the stereospecific assignment of the isopropyl groups of Val and Leu presented here, the [2-<sup>13</sup>C]Glc labeling scheme has proven to be a remarkably versatile scheme, and should therefore become an attractive tool for structural investigations of proteins by ssNMR.

### 4. Materials and methods

#### 4.1. Sample preparation

[U-<sup>13</sup>C]Glc- and [2-<sup>13</sup>C]Glc-labeled T3SS PrgI needles were prepared as described in Loquet et al. [10]. [U-<sup>13</sup>C]Glc- and [2-<sup>13</sup>C]Glc-labeled ubiquitin was prepared as described in Seidel et al. [30]. [2-<sup>13</sup>C]-Glc-labeled PrgI protomers were prepared as in Loquet et al. [10] with the exception that the monomers were not polymerized. The buffer used for the solution NMR studies contained 20 mM MES, pH 5.5, 10% D<sub>2</sub>O. All samples were uniformly <sup>15</sup>N labeled.

#### 4.2. Solid-state NMR experiments and data processing

Samples were packed in 4 mm MAS rotors, using protein quantities of ~10 mg for T3SS PrgI needles and ~20 mg for ubiquitin. All spectra were recorded at a spinning frequency of 11 kHz and the <sup>13</sup>C chemical shifts were calibrated with DSS as an internal Ref. [31]. The temperature-dependent position of the water proton resonance was used to measure the temperature inside the MAS rotor [32]. High-power <sup>1</sup>H–<sup>13</sup>C decoupling (SPINAL-64 [33]) with a radio-frequency amplitude of 83 kHz was applied during evolution and detection periods.

For [U-<sup>13</sup>C]Glc- and [2-<sup>13</sup>C]Glc-labeled T3SS PrgI needles, two-dimensional <sup>13</sup>C–<sup>13</sup>C ssNMR experiments were conducted on a 20.0 Tesla (<sup>1</sup>H resonance frequency: 850 MHz) wide-bore spectrometer (Bruker Biospin, Germany), equipped with a 4 mm triple-resonance (<sup>1</sup>H, <sup>13</sup>C, <sup>15</sup>N) MAS probe. The experiments were conducted at a sample temperature of 278 K (+5 °C). <sup>13</sup>C–<sup>13</sup>C transfer was achieved via proton-driven spin-diffusion (PDS) with mixing times of 50 ms and 400 ms for [U-<sup>13</sup>C]Glc- and [2-<sup>13</sup>C]Glc-labeled PrgI needles, respectively. These two spectra were processed with NMRpipe [34] and analyzed using CcpNmr [35].

For [U-<sup>13</sup>C]Glc- and [2-<sup>13</sup>C]Glc-labeled ubiquitin, two-dimensional <sup>13</sup>C–<sup>13</sup>C ssNMR experiments were conducted on a 18.8 Tesla (<sup>1</sup>H resonance frequency: 800 MHz) standard-bore

spectrometer (Bruker Biospin, Germany), equipped with a 4 mm triple-resonance (<sup>1</sup>H, <sup>13</sup>C, <sup>15</sup>N) MAS probe. <sup>13</sup>C–<sup>13</sup>C transfer was achieved via proton-driven spin-diffusion (PDS) with mixing times of 50 ms and 100 ms for [U-<sup>13</sup>C]Glc- and [2-<sup>13</sup>C]Glc-labeled ubiquitin, respectively. The spectra were processed with Topspin (Bruker Biospin, Germany) and analyzed in SPARKY version 3.1 (T.D. Goddard & D.G. Kneller, University of California).

#### 4.3. Solution NMR experiment and data processing

A <sup>1</sup>H–<sup>13</sup>C HSQC spectrum was recorded on a 21.1 Tesla (<sup>1</sup>H resonance frequency: 900 MHz) standard-bore spectrometer (Bruker Biospin, Germany), equipped with a cryogenically-cooled triple resonance probe head, with 1024 (*t*<sub>2</sub>) × 1152 (*t*<sub>1</sub>) complex points and maximum acquisition times of 33.6 ms (*t*<sub>2</sub>) and 33.9 ms (*t*<sub>1</sub>). 32 scans were collected per indirect increment. The <sup>1</sup>H carrier frequency was set to the water resonance (4.67 ppm), and the <sup>13</sup>C carrier frequency was set to 45 ppm. The spectrum was zero-filled automatically, apodized with a squared sine bell window function along *t*<sub>2</sub> and *t*<sub>1</sub> axes, and then Fourier transformed. The spectrum was processed with NMRpipe [34] and analyzed using SPARKY version 3.1 (T.D. Goddard & D.G. Kneller, University of California).

### Acknowledgments

We are grateful to Christian Griesinger for continuous support of this project, Zrinka Gattin for discussions, and Gitta Angerstein for expert technical assistance. We thank the Max Planck Society, the DFG (Emmy Noether fellowship to A. Lange), the China Scholarship Council (Ph.D. scholarship to G. Lv), and EMBO (long-term fellowship to A. Loquet) for financial support.

### Appendix A. Supplementary data

HSQC spectrum of T3SS PrgI protomers; glycolysis and PPP pathways involved in the formation of pyruvate; 1D traces for residues Val65 and Val67 in PrgI; the stereospecific assignment of Val and Leu in ubiquitin. Supplementary data associated with this article can be found, in the online version, at <http://dx.doi.org/10.1016/j.jmr.2012.12.017>.

### References

- [1] P. Guntert, W. Braun, M. Billeter, K. Wuthrich, Automated stereospecific <sup>1</sup>H-NMR assignments and their impact on the precision of protein-structure determinations in solution, *J. Am. Chem. Soc.* 111 (1989) 3997–4004.
- [2] D. Neri, T. Szyperski, G. Otting, H. Senn, K. Wuthrich, Stereospecific nuclear magnetic resonance assignments of the methyl groups of valine and leucine in the DNA-binding domain of the 434 repressor by biosynthetically directed fractional <sup>13</sup>C labeling, *Biochemistry* 28 (1989) 7510–7516.
- [3] M. Kainosho, T. Torizawa, Y. Iwashita, T. Terauchi, A. Mei Ono, P. Guntert, Optimal isotope labelling for NMR protein structure determinations, *Nature* 440 (2006) 52–57.
- [4] P.C. Driscoll, A.M. Gronenborn, G.M. Clore, The influence of stereospecific assignments on the determination of three-dimensional structures of proteins by nuclear magnetic resonance spectroscopy. Application to the sea anemone protein BDS-I, *FEBS Lett.* 243 (1989) 223–233.
- [5] J. Janin, S. Miller, C. Chothia, Surface, subunit interfaces and interior of oligomeric proteins, *J. Mol. Biol.* 204 (1988) 155–164.
- [6] D.F. Hansen, L.E. Kay, Determining valine side-chain rotamer conformations in proteins from methyl <sup>13</sup>C chemical shifts: application to the 360 kDa half-proteasome, *J. Am. Chem. Soc.* 133 (2011) 8272–8281.
- [7] M. Hong, T.V. Mishanina, S.D. Cady, Accurate measurement of methyl <sup>13</sup>C chemical shifts by solid-state NMR for the determination of protein side chain conformation: the influenza A M2 transmembrane peptide as an example, *J. Am. Chem. Soc.* 131 (2009) 7806–7816.
- [8] F. Castellani, B. van Rossum, A. Diehl, M. Schubert, K. Rehbein, H. Oschkinat, Structure of a protein determined by solid-state magic-angle-spinning NMR spectroscopy, *Nature* 420 (2002) 98–102.
- [9] C. Wasmer, A. Lange, H. Van Melckebeke, A.B. Siemer, R. Riek, B.H. Meier, Amyloid fibrils of the HET-s(218–289) prion form a  $\beta$ -solenoïd with a triangular hydrophobic core, *Science* 319 (2008) 1523–1526.

- [10] A. Loquet, N.G. Sgourakis, R. Gupta, K. Giller, D. Riedel, C. Goosmann, C. Griesinger, M. Kolbe, D. Baker, S. Becker, A. Lange, Atomic model of the type III secretion system needle, *Nature* 486 (2012) 276–279.
- [11] S.D. Cady, K. Schmidt-Rohr, J. Wang, C.S. Soto, W.F. Degrado, M. Hong, Structure of the amantadine binding site of influenza M2 proton channels in lipid bilayers, *Nature* 463 (2010) 689–692.
- [12] A. Lange, K. Giller, S. Hornig, M.F. Martin-Eauclaire, O. Pongs, S. Becker, M. Baldus, Toxin-induced conformational changes in a potassium channel revealed by solid-state NMR, *Nature* 440 (2006) 959–962.
- [13] H.S. Atreya, K.V. Chary, Selective 'unlabeling' of amino acids in fractionally  $^{13}\text{C}$  labeled proteins: an approach for stereospecific NMR assignments of  $\text{CH}_3$  groups in Val and Leu residues, *J. Biomol. NMR* 19 (2001) 267–272.
- [14] G. Ostler, A. Soteriou, C.M. Moody, J.A. Khan, B. Birdsall, M.D. Carr, D.W. Young, J. Feeney, Stereospecific assignments of the leucine methyl resonances in the  $^1\text{H}$  NMR spectrum of *Lactobacillus casei* dihydrofolate reductase, *FEBS Lett.* 318 (1993) 177–180.
- [15] M.J. Plevin, O. Hamelin, J. Boisbouvier, P. Gans, A simple biosynthetic method for stereospecific resonance assignment of prochiral methyl groups in proteins, *J. Biomol. NMR* 49 (2011) 61–67.
- [16] V. Tugarinov, L.E. Kay, Stereospecific NMR assignments of prochiral methyls, rotameric states and dynamics of valine residues in malate synthase G, *J. Am. Chem. Soc.* 126 (2004) 9827–9836.
- [17] P. Gans, O. Hamelin, R. Sounier, I. Ayala, M.A. Dura, C.D. Amero, M. Noirclerc-Savoye, B. Franzetti, M.J. Plevin, J. Boisbouvier, Stereospecific isotopic labeling of methyl groups for NMR spectroscopic studies of high-molecular-weight proteins, *Angew Chem. Int. Ed. Engl.* 49 (2010) 1958–1962.
- [18] H. Senn, B. Werner, B.A. Messerle, C. Weber, R. Traber, K. Wuthrich, Stereospecific assignment of the methyl  $^1\text{H}$ -NMR lines of valine and leucine in polypeptides by nonrandom  $^{13}\text{C}$  labeling, *FEBS Lett.* 249 (1989) 113–118.
- [19] D. Neri, G. Otting, K. Wuthrich,  $^1\text{H}$  and  $^{13}\text{C}$  NMR chemical-shifts of the diastereotopic methyl-groups of valyl and leucyl residues in peptides and proteins, *Tetrahedron* 46 (1990) 3287–3296.
- [20] M. Schubert, T. Manolikas, M. Rogowski, B.H. Meier, Solid-state NMR spectroscopy of 10%  $^{13}\text{C}$  labeled ubiquitin: spectral simplification and stereospecific assignment of isopropyl groups, *J. Biomol. NMR* 35 (2006) 167–173.
- [21] A. Loquet, K. Giller, S. Becker, A. Lange, Supramolecular interactions probed by  $^{13}\text{C}$ - $^{13}\text{C}$  solid-state NMR spectroscopy, *J. Am. Chem. Soc.* 132 (2010) 15164–15166.
- [22] P. Lundstrom, K. Teilum, T. Carstensen, I. Bezsonova, S. Wiesner, D.F. Hansen, T.L. Religa, M. Akke, L.E. Kay, Fractional  $^{13}\text{C}$  enrichment of isolated carbons using  $[1-^{13}\text{C}]$ - or  $[2-^{13}\text{C}]$ -glucose facilitates the accurate measurement of dynamics at backbone  $\text{C}\alpha$  and side-chain methyl positions in proteins, *J. Biomol. NMR* 38 (2007) 199–212.
- [23] A. Loquet, G. Lv, K. Giller, S. Becker, A. Lange,  $^{13}\text{C}$  spin dilution for simplified and complete solid-state NMR resonance assignment of insoluble biological assemblies, *J. Am. Chem. Soc.* 133 (2011) 4722–4725.
- [24] D. Voet, J.G. Voet, *Biochemistry*, John Wiley & Sons, Inc., Berlin, 2011.
- [25] E.M. Brekke, A.B. Walls, A. Schousboe, H.S. Waagepetersen, U. Sonnewald, Quantitative importance of the pentose phosphate pathway determined by incorporation of  $^{13}\text{C}$  from  $[2-^{13}\text{C}]$ - and  $[3-^{13}\text{C}]$ -glucose into TCA cycle intermediates and neurotransmitter amino acids in functionally intact neurons, *J. Cereb. Blood Flow Metab.* 32 (2012) 1788–1799.
- [26] P. Lundstrom, D.F. Hansen, L.E. Kay, Measurement of carbonyl chemical shifts of excited protein states by relaxation dispersion NMR spectroscopy: comparison between uniformly and selectively  $^{13}\text{C}$  labeled samples, *J. Biomol. NMR* 42 (2008) 35–47.
- [27] C. Guo, V. Tugarinov, Selective  $^1\text{H}$ - $^{13}\text{C}$  NMR spectroscopy of methyl groups in residually protonated samples of large proteins, *J. Biomol. NMR* 46 (2009) 127–133.
- [28] T. Szyperski, Biosynthetically directed fractional  $^{13}\text{C}$ -labeling of proteinogenic amino acids. An efficient analytical tool to investigate intermediary metabolism, *Eur. J. Biochem.* 232 (1995) 433–448.
- [29] G. Lv, A. Kumar, K. Giller, M.L. Orcellet, D. Riedel, C.O. Fernandez, S. Becker, A. Lange, Structural comparison of mouse and human  $\alpha$ -synuclein amyloid fibrils by solid-state NMR, *J. Mol. Biol.* 420 (2012) 99–111.
- [30] K. Seidel, M. Eitzkorn, H. Heise, S. Becker, M. Baldus, High-resolution solid-state NMR studies on uniformly  $[^{13}\text{C}, ^{15}\text{N}]$ -labeled ubiquitin, *Chembiochem* 6 (2005) 1638–1647.
- [31] J.L. Markley, A. Bax, Y. Arata, C.W. Hilbers, R. Kaptein, B.D. Sykes, P.E. Wright, K. Wuthrich, Recommendations for the presentation of NMR structures of proteins and nucleic acids—IUPAC-IUBMB-IUPAB Inter-Union Task Group on the standardization of data bases of protein and nucleic acid structures determined by NMR spectroscopy, *Eur. J. Biochem.* 256 (1998) 1–15.
- [32] A. Bockmann, C. Gardiennet, R. Verel, A. Hunkeler, A. Loquet, G. Pintacuda, L. Emsley, B.H. Meier, A. Lesage, Characterization of different water pools in solid-state NMR protein samples, *J. Biomol. NMR* 45 (2009) 319–327.
- [33] B.M. Fung, A.K. Khitrin, K. Ermolaev, An improved broadband decoupling sequence for liquid crystals and solids, *J. Magn. Reson.* 142 (2000) 97–101.
- [34] F. Delaglio, S. Grzesiek, G.W. Vuister, G. Zhu, J. Pfeifer, A. Bax, NMRPipe: a multidimensional spectral processing system based on UNIX pipes, *J. Biomol. NMR* 6 (1995) 277–293.
- [35] W.F. Vranken, W. Boucher, T.J. Stevens, R.H. Fogh, A. Pajon, M. Llinas, E.L. Ulrich, J.L. Markley, J. Ionides, E.D. Laue, The CCPN data model for NMR spectroscopy: development of a software pipeline, *Proteins* 59 (2005) 687–696.